TITLE

Rhythmic temporal coordination of neural activity avoids representational conflict during working memory

AUTHORS

Miral Abdalaziz[1,2], Zach V. Redding[1,2], Ian C. Fiebelkorn[1]*

[2]These authors contributed equally

CORRESPONDING AUTHOR

*Ian C. Fiebelkorn (email: Ian_Fiebelkorn@URMC.Rochester.edu)

AFFILIATIONS

[1]Department of Neuroscience and Delmonte Institute for Neuroscience, University of Rochester, Rochester, NY 14627, USA

SUMMARY

Selective attention[1] includes alternating states associated with either attentional sampling or attentional shifting, helping to avoid functional conflicts by isolating function-specific neural activity in time[2-4]. We hypothesized that such rhythmic temporal coordination might also help to avoid representational conflicts during working memory[5]. Multiple items can be simultaneously held in working memory, and these items can be represented by overlapping neural populations[6-8]. Traditional theories propose that short-term storage of to-be-remembered items occurs through persistent neural activity[9-11], but when neurons are simultaneously representing multiple items, persistent activity creates a potential for representational conflicts. In comparison, more recent, 'activity-silent' theories of working memory propose that items are stored through short-term changes in synaptic weights[12-15]. Transient bursts in neural activity[16], rather than persistent activity, would serve to refresh these short-term synaptic changes. Here, we used EEG and response times (RTs) to test whether rhythmic temporal coordination helps to isolate neural activity associated with different to-be-remembered items, thereby avoiding representational conflicts. Consistent with this hypothesis, we report that the relative strength of different item representations alternates over time as a function of frequency-specific phase. Although RTs were linked to theta (~6Hz) and beta (~25 Hz) phase during a memory delay, the relative strength of item representations only alternated as a function of beta phase. The present findings support 'activity-silent' theories of working memory[9,12,14], and inform models describing the role of oscillatory dynamics in organizing working memory[17-20]. Finally, these findings support rhythmic temporal coordination as a general mechanism for avoiding either functional or representational conflicts during cognitive processes.

RESULTS

The rhythmic coordination of neural activity can help to isolate competing functions or information in time[21-26]. For example, previous studies have provided evidence that selective attention is characterized by rhythmically alternating states (at ~4–6 Hz) associated with potentially conflicting functions: attentional sampling (i.e., sensory functions of the attention network) and attentional shifting (i.e., motor functions of the attention network)[3,4,27-29]. Here, we tested whether such rhythmic temporal coordination of neural activity is a more general mechanism for avoiding conflict during cognitive processes. Specifically, we tested whether rhythmic temporal coordination helps to avoid potential *representational conflicts* during working memory.

Working memory is the process through which behaviorally relevant information is temporarily stored and internally sampled[5,30]. Traditional theories of working memory have proposed that the short-term storage of information occurs through persistent neural activity (i.e., increased neural activity that spans the entire memory delay)[9]. While there is clear evidence of increased neural activity during working memory delays[9-11,31], short-term storage through persistent neural activity becomes potentially problematic when there are multiple to-be-remembered items. Previous evidence has demonstrated that different to-be-remembered items can be simultaneously represented by *overlapping* neural populations[6-8,32]. Under such conditions, short-term storage through persistent neural activity could lead to representational conflicts. So how can overlapping neural populations simultaneously represent multiple to-be-remembered items, avoiding representational conflicts that might arise from persistent neural activity?

More recent, 'activity-silent' theories of working memory propose that the storage of to-be-remembered items occurs, in part, through short-term changes in synaptic weights[12-15]. Transient bursts in neural activity, rather than persistent neural activity, would serve to refresh these short-term synaptic changes. In fact, recent studies have demonstrated that working memory delays are characterized by transient bursts of beta- (20–35 Hz) and gamma-band (45–100 Hz) activity[14,16,33]. Here, we used high-density EEG (128 channels) and response times (RTs) to investigate whether rhythmic temporal coordination—like that previously observed during selective attention[3,4]—helps to organize transient neural activity associated with different to-be-remembered items. Rhythmic temporal coordination of neural activity would thereby help to avoid representational conflicts during working memory. Based on the notion that different item representations are consistently refreshed at different oscillatory phases, we specifically predicted that the relative strength of simultaneously held item representations would alternate over time as a function of oscillatory phase (Fig. 1D). Consistent with this prediction, previous theoretical models of working memory have proposed that serially presented, to-be-remembered items are multiplexed at different phases of frequency-specific neural activity[17,34,35]. Supporting evidence for these theoretical models comes from intracranial data in both humans[19,20] and monkeys[18]. For example, Bahramisharif *et al.* [19]

reported a link between item-specific high-frequency band activity (75–120 Hz)—a proxy for population spiking[36]—and the phase of theta/alpha (7–13 Hz) oscillations. The specific phase associated with changes in item-specific high-frequency band activity was dependent on when an item occurred within a sequence of to-be-remembered items.

Here, we used an experimental task with simultaneously presented to-be-remembered items (Fig. 1A). The Research Subjects Review Board at the University of Rochester approved the study protocol. On each trial, differently oriented gratings (i.e., either horizontal, vertical, or diagonal) were presented 4 degrees from central fixation, on both the right and the left. Shortly after the presentation of these two memory items (i.e., to-be-remembered items), a task-irrelevant flash event was presented at the same location as one of the previously presented items (with equal probability). Here, we hypothesized that the relative strength of the item representations (i.e., neural representations of the to-be-remembered items) would alternate in time as a function of oscillatory phase (Fig. 1D). We included the flash event to create a consistent pattern of alternation across trials (e.g., Item 1, Item 2, Item 1…)[37-39]. Following a variable delay, participants (n = 22) reported, as quickly and as accurately as possible, whether a subsequent probe matched the memory item presented to (1) the left of fixation (40% of trials), (2) the right of fixation (40% of trials), or (3) neither of those memory items (20% of trials). The memory probe was presented at a neutral location, four degrees above central fixation. We defined 'Item 1' trials as those trials when the probe matched the memory item presented on the same side of fixation as the flash event, and 'Item 2' trials as those trials when the probe matched the memory item presented on the opposite side of fixation from the flash event (Fig. 1B).

Participants were able to perform the experimental task with high accuracy (mean = 85.2%, SE = 2.8). For the remaining analyses, we used RTs on correct trials as the behavioral measure (Fig. 1C). A two-way repeated measures ANOVA revealed a main effect for the item condition (i.e., Item 1, Item 2, or Neither, $p < 0.001$), no main effect for the flash condition (i.e., flash left or flash right, $p = 0.31$), and no interaction between the conditions ($p = 0.68$). Based on these results, we combined trials when the flash event occurred on either the right or left of central fixation. Follow-up t-tests revealed that RTs for both the Item 1 ($p < 0.001$) and the Item 2 ($p < 0.001$) conditions were significantly faster than RTs for the Neither condition, while RTs were not significantly different between the Item 1 and Item 2 conditions ($p = 0.21$).

We next tested whether behavioral performance was linked to the phase of frequency-specific neural activity during the memory delay[28,40,41], first combining all trials for which the memory probe was a match for either of the two memory items (i.e., combining the Item 1 and Item 2 conditions). We binned trials based on oscillatory phase just prior to when the memory probe was presented and then averaged z-standardized RTs (for each participant) within overlapping, 90-degree phase bins (with a step size of 10 degrees). Figure 2A shows RTs as a function of phase (i.e., a resulting phase-RT function) for a single electrode and frequency, averaged across all participants

(n = 22). We hypothesized that phase bins associated with peaks (i.e., slower RTs) and troughs (i.e., faster RTs) in behavioral performance would be separated by approximately 180 degrees. Based on this hypothesis, we fit the phase-RT functions with a one-cycle sine wave (Fig. 2A) and used the amplitude of that sine wave to measure the strength of the relationship between frequency-specific oscillatory phase and RTs[28,40,41]. Figure 2B shows the amplitude of these fitted sine waves (i.e., the strength of the phase-RT relationships) for all electrode and frequency combinations (from 1–55 Hz), with statistically insignificant values set to zero. Statistical significance was based on a permutation test (see Methods). There were clusters of significant phase-RT relationships ($p < 0.05$, after correcting for multiple comparisons) in the theta (3–8 Hz) and beta bands (15–35 Hz), centered at approximately 6 Hz and 25 Hz, respectively. Theta- and beta-band activity have been previously linked to cognitive control[42,43] and the maintenance[18,20,43-46] of items held in working memory. Figure 2C shows scalp topographies for the electrodes with significant phase-RT relationships at 6 Hz and 25 Hz. Importantly, we also found consistent phase-RT relationships in the theta and beta bands when we subsequently split the data into the Item 1 and Item 2 conditions (Fig. 2D). Figure 2E shows all of the electrode and frequency combinations where we observed statistically significant phase-RT relationships for both the Item 1 and the Item 2 conditions, at either $p < 0.05$ or $p < 0.1$ (after corrections for multiple comparisons). The present results demonstrate that behavioral performance during a working memory task fluctuates over time as a function of oscillatory phase within multiple frequency bands.

We then used the item-specific phase-RT relationships to investigate whether the relative strength of the different item representations alternated in time as a function of oscillatory phase (Fig. 1D). Here, we tested whether the specific phases associated with better and worse behavioral performance were different for the Item 1 and Item 2 conditions (Fig. 3A). We again fit the participant-level phase-RT functions with one-cycle sine waves, but we now measured the phase of those sine-wave fits rather than the amplitude. We used a circular Watson-Williams test[47] to determine whether the distributions of participant-level phases (i.e., the phase of the sine-wave fits) were different between the Item 1 and Item 2 conditions. We only tested for between-condition phase differences at electrode and frequency combinations where we previously detected significant phase-RT relationships for both the Item 1 and the Item 2 conditions (Fig. 2E). That is, we only made between-condition comparisons when both the Item 1 and the Item 2 conditions demonstrated a relationship between oscillatory phase and behavioral performance. Figure 3B shows the condition-specific phase distributions and angular means for a representative electrode and frequency. Figures 3C and 3D show all of the statistically significant ($p < 0.05$, after correction for multiple comparisons) electrode and frequency combinations, as well as the mean differences in phase between the Item 1 and Item 2 conditions. That is, the mean difference in the angular shift of the phase-RT functions between the Item 1 and Item 2 conditions. The analysis associated with the results shown in Figure 3C included all of the electrodes (e.g., 14 electrodes at 25 Hz) with

significant phase-RT relationships at the $p < 0.05$ level for both the Item 1 and the Item 2 conditions (Fig. 2E), and the analysis associated with the results shown in Figure 3D included all of the electrodes (e.g., 33 electrodes at 25 Hz) with significant phase-RT relationships at the $p < 0.1$ level for both the Item 1 and the Item 2 conditions (Fig. 2E). The specific beta phases associated with better or worse behavioral performance were different for the Item 1 and Item 2 conditions. These findings are consistent with the hypothesis that the relative strength of different item representations alternates over time as a function of oscillatory phase (Fig. 1D). In comparison, we found no difference in the specific theta phases associated with better or worse behavioral performance between the Item 1 and Item 2 conditions (Fig. 3), despite earlier results demonstrating that RTs fluctuate over time as a function of theta phase (Fig. 2). Siegel *et al.* [18] reported a similar pattern of results in the prefrontal cortex of monkeys, measuring information encoded by spiking activity as a function of oscillatory phase (rather than behavioral performance as a function of oscillatory phase). While information coding in spiking activity generally fluctuated as a function of both theta phase and beta phase, the optimal encoding of different items only varied as a function of beta phase. That is, there was no theta-band difference in the optimal encoding phase for different to-be-remembered items.

A prominent model of oscillatory dynamics during working memory has proposed that theta-band activity coordinates item-specific higher-frequency activity[17,34]. According to this model, each cycle of the theta-dependent, higher frequency activity refreshes the representation of a different to-be-remembered item (see Bahramisharif *et al.* [19] for supporting data). The number of cycles of the higher-frequency activity, nested within theta-band activity, might therefore reflect the number of to-be-remembered items. The present findings, as well as those from Siegel *et al.* [18], instead indicate that each to-be-remembered item is refreshed within a *single* cycle of the higher frequency activity (i.e., within a single cycle of beta-band activity).

To test whether theta- and beta-band activity might be functionally linked in the present data, we measured whether beta amplitude varied as a function of theta phase (i.e., we measured phase-amplitude coupling[48,49]). Here, we used the same approach used to estimate phase-RT relationships. We calculated average amplitude (from 15–55 Hz) in overlapping theta-phase bins and fit the resulting phase-amplitude functions with one-cycle sine waves to measure the strength of the relationship (Fig. 4A)[28]. We specifically binned higher-frequency amplitude using theta phase (at 6 Hz) from the electrode (i.e., D14) where we previously measured the strongest phase-RT relationship (Fig. 2). Figure 4B shows the strength of phase-amplitude coupling (i.e., the amplitude of the sine-wave fits) for all of the statistically significant electrode and frequency combinations ($p < 0.05$ after corrections for multiple comparisons), with significant values clustered in the beta band. Figure 4C shows the scalp topography of the electrodes with significant coupling between theta phase (at 6Hz) and beta amplitude (at 25 Hz). These findings demonstrate that beta amplitude fluctuates as a function of theta phase. Such theta-dependent fluctuations in beta

amplitude are consistent with previously described, transient changes in beta-band activity during a working memory delay, rather than persistent changes in beta-band activity[14,16].

Figure 4A shows a representative phase-amplitude function from a single electrode, with beta amplitude peaking when theta phase is at approximately 180 degrees, which is the same theta phase associated with relatively worse behavioral performance (Fig. 2A). This pattern of results fits with 'activity-silent' theories of working memory[12-15]. If increased beta-band activity reflects transient neural activity that refreshes short-term synaptic changes, it should be most likely to occur when changes in synaptic weights are beginning to decay and behavioral performance is therefore at its worst (i.e., when item representations need to be refreshed).

The scalp topographies of our results are similar to previous EEG investigations of working memory. Supplemental Figure 1 shows the scalp topographies of isolated periodic components[50] for the frequencies of interest during the memory delay (i.e., 6 Hz and 25 Hz). Theta-band activity in the present EEG results is consistent with frontal midline theta (FMT)[44], which is thought to originate in medial prefrontal and anterior cingulate cortices[42,51]. FMT has been linked, for example, to memory capacity[43] and behavioral performance[52,53] during working memory tasks. Ratcliffe *et al.* [43] recently provided evidence that FMT coordinates the maintenance of working memory content in posterior brain regions[30], and neural synchronization is commonly observed between frontal and parietal cortices during working memory tasks[54-58]. Such neural synchronization can occur within both the theta and the beta bands[28,54-58], consistent with the behaviorally relevant frequencies observed during the present working memory task (Figs. 2–4).

Theta-band activity within frontal and parietal cortices also temporally coordinates rhythmically alternating states associated with either attentional sampling or shifting, helping to avoid potential functional conflicts[3,28]. The present results demonstrate that such rhythmic temporal coordination of neural activity is a more general mechanism for avoiding conflicts during cognitive processes, providing evidence that it also helps to avoid potential representational conflicts during working memory. Our findings show that behavioral performance during working memory, like that during selective attention[27,28,41], fluctuates as a function of both theta phase and beta phase. Rhythmic temporal coordination of competing attentional states, however, seems to occur within the theta band (but not the beta band), whereas rhythmic temporal coordination of competing item representations occurs within the beta band (but not the theta band). Future research will be needed to test whether the behaviorally relevant, frequency-specific neural activity associated with selective attention (i.e., external sampling) and working memory (i.e., internal sampling) share common neural sources.

FIGURES

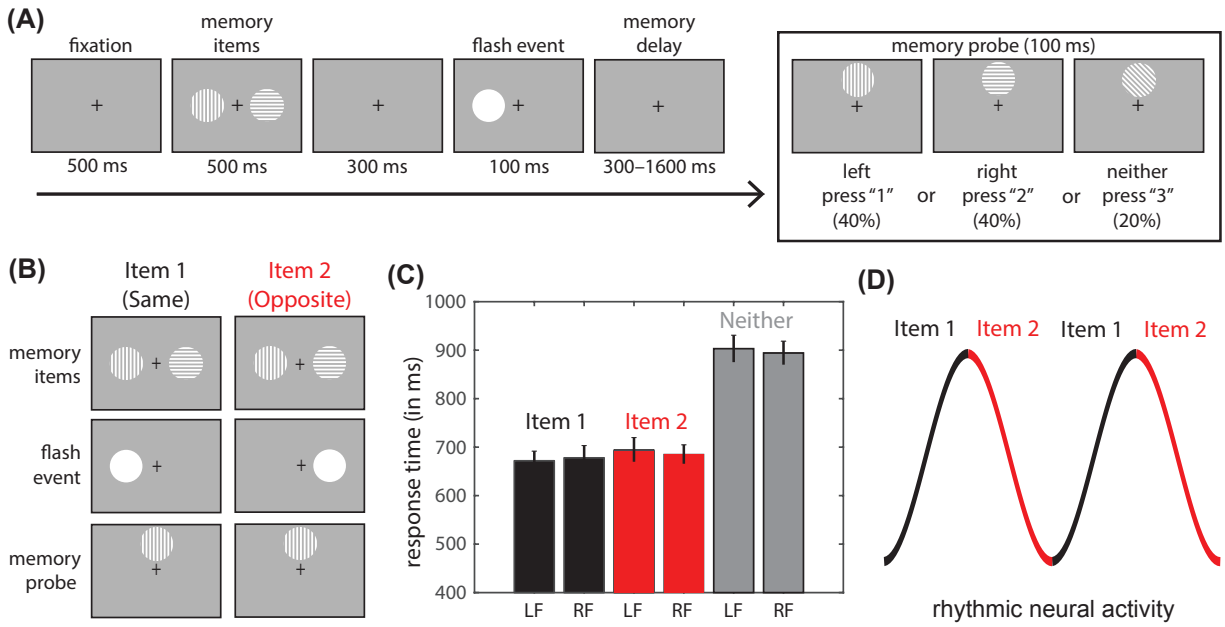

Figure 1. *Behavioral performance during a working memory task.* (A) Participants determined whether a probe was a match for either of two previously presented memory items. (B) We defined 'Item 1' trials as those trials when the probe matched the memory item presented on the same side of space as an intervening flash event and 'Item 2' trials as those trials when the probe matched the memory item presented on the opposite side of space as an intervening flash event. (C) Participants were faster to respond when the probe matched either of the previously presented memory items, relative to when the probe matched neither memory item. (D) We hypothesized that the relative strength of the representations for Item 1 and Item 2 would alternate in time as a function of oscillatory phase.

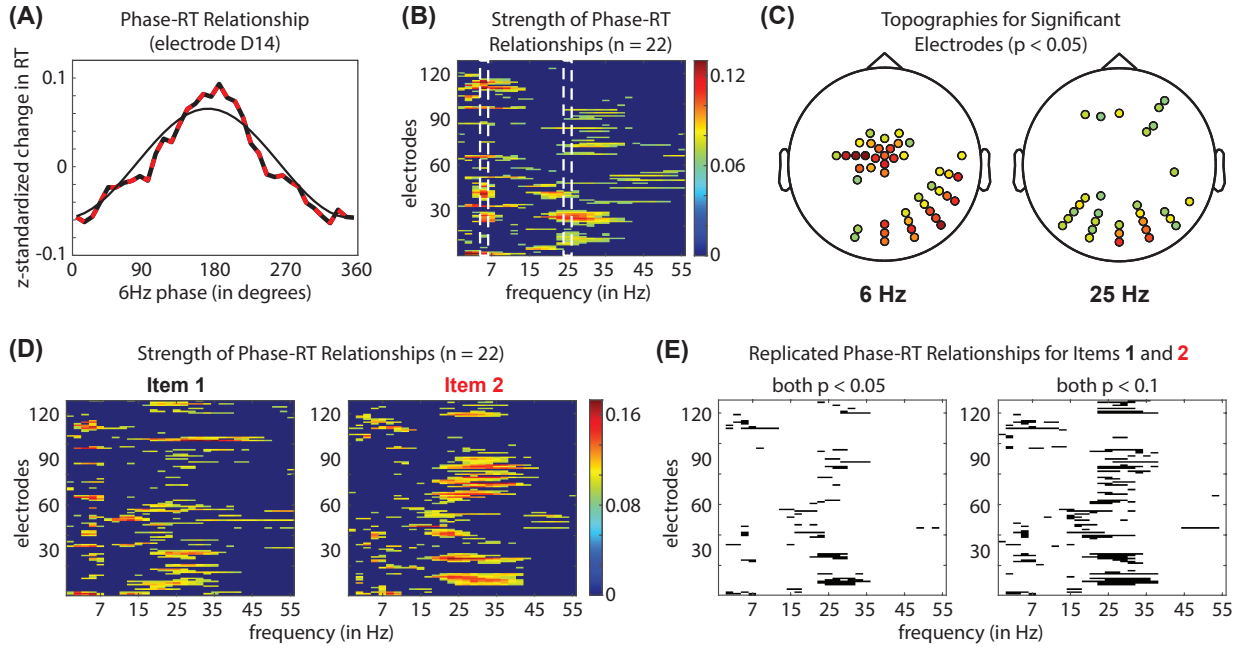

Figure 2. *Response times (RTs) fluctuated as a function of theta and beta phase.* (A) Shows RTs as a function of oscillatory phase (at 6 Hz) for a single representative electrode (alternating red/black line), including all trials when the probe was a match for either of the two memory items (i.e., combining the Item 1 and Item 2 trials). We used the amplitude of a fitted, one-cycle sine wave (solid black line) to measure the strength of the phase-RT relationship. (B) Shows the strength of statistically significant ($p < 0.05$) phase-RT relationships for all of the electrode and frequency combinations. Statistically insignificant results were set to zero. There were clusters of significant results in both the theta and the beta bands, with (C) showing the scalp topographies of electrodes with significant phase-RT relationships within the theta (at 6Hz) and beta (at 25 Hz) bands. (D) Results were consistent when calculated separately for the Item 1 and Item 2 conditions, with (E) overlapping, statistically significant results in the theta and beta bands.

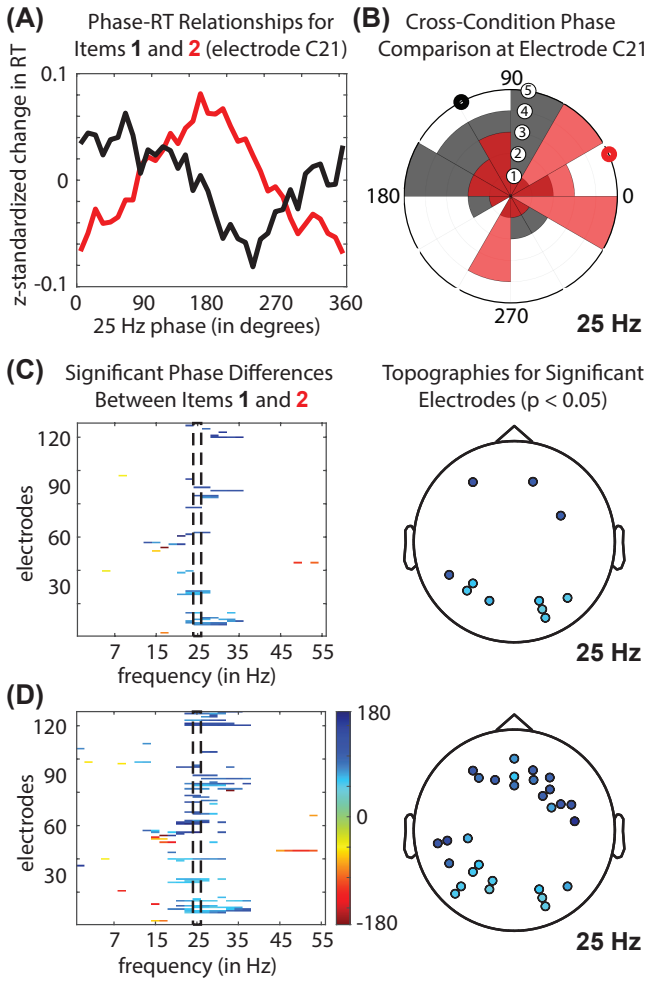

Figure 3. *The phases associated with faster and slower response times (RTs) were different for the Item 1 and Item 2 conditions.* (A) Shows RTs as a function of oscillatory phase (at 25 Hz), separately for the Item 1 (black line) and Item 2 (red line) conditions, for a single representative electrode. (B) Shows circular histograms, plotting the phase of fitted one-cycle sine waves (see Fig. 2A) for each participant's phase-RT functions (n = 22), separately for the Item 1 and Item 2 conditions. These results are shown for a single representative electrode, with the angular mean phases (n = 22) for each condition plotted as black (Item 1) and red (Item 2) circles. (C and D) Show all electrode and frequency combinations where the phases associated with faster and slower RTs were significantly different between the Item 1 and Item 2 conditions ($p < 0.05$), including the scalp topographies of electrodes with significant effects in the beta band (at 25 Hz). The color code represents the mean angular difference in phase between the Item 1 and Item 2 conditions. The analyses shown in (C) included all electrodes where we previously observed significant phase-RT relationships in both the Item 1 and the Item 2 conditions at the $p < 0.05$ level (see Figure 2E), while those shown in (D) included all electrodes where we previously observed significant phase-RT relationships in both the Item 1 and the Item 2 conditions at the $p < 0.1$ level (see Figure 2E).

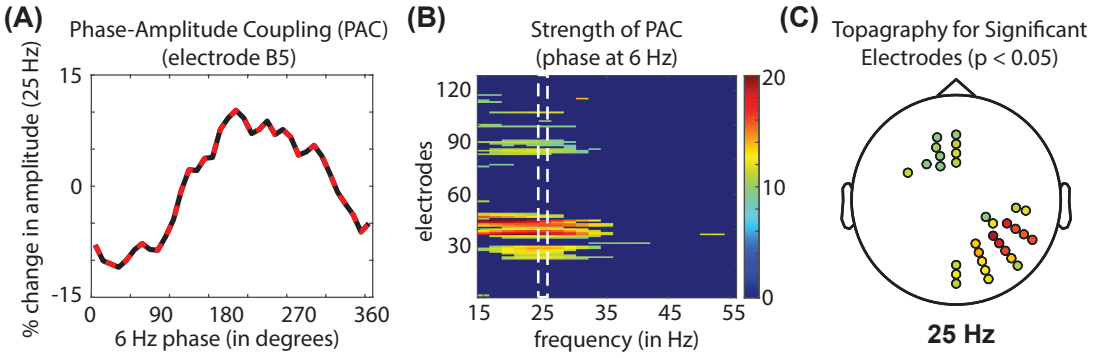

Figure 4. *The amplitude of beta-band activity fluctuates as a function of theta phase.* (A) Shows beta amplitude as a function of theta phase (at 6 Hz) for a single representative electrode (alternating red/black line), including all trials when the probe was a match for either of the two memory items (i.e., combining the Item 1 and Item 2 trials). We used the amplitude of a fitted, one-cycle sine wave to measure the strength of the phase-amplitude relationship (see Fig. 2A). (B) Shows the strength of statistically significant ($p < 0.05$) phase-amplitude relationships for all of the electrode and frequency combinations. Statistically insignificant results were set to zero. For all phase-amplitude calculations, we used theta phase from the electrode that had the strongest phase-RT relationship (see Fig. 2). There was a cluster of significant phase-amplitude results in the beta band, with (C) showing the scalp topography of electrodes with significant phase-amplitude relationships within the beta band (at 25 Hz).

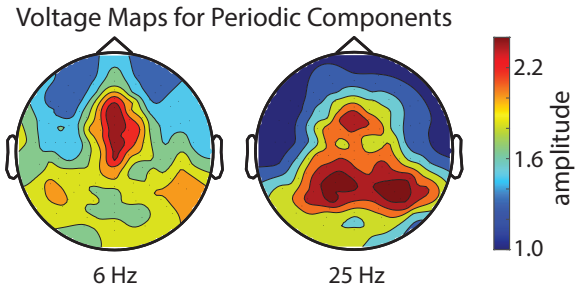

Supplemental Figure 1. *Scalp topographies of the isolated periodic components within the theta and beta bands.* We used the FOOOF algorithm[50] to remove the aperiodic, 1/f component, isolating the periodic components at behaviorally relevant frequencies. These scalp topographies are consistent with previous EEG studies that measured theta- and beta-band activity during a working memory delay.

METHODS

Contact for Resource Sharing

Further information and requests for code or data should be directed to and will be fulfilled by the Lead Contact, Ian C. Fiebelkorn (Ian_Fiebelkorn@URMC.Rochester.edu).

Subject Details

Twenty-seven individuals (12 females; 18–42 years old) with normal or corrected-to-normal vision and no history of neurological disease participated in the experiment. The Research Subjects Review Board at the University of Rochester approved the study protocol. Written informed consent was obtained from all participants prior to data collection, in line with the Declaration of Helsinki. Five participants were excluded from the analyses because of excessive blinks and/or eye movements (i.e., on greater than 20 percent of trials).

Behavioral Task and Behavioral Data

Figure 1 summarizes our experimental design. The experiment was administered in a light- and sound-attenuated chamber. Presentation software (Neurobehavioral Systems, Albany, CA, USA) was used to control stimuli and monitor responses. The visual stimuli were presented on a 24-inch LCD monitor (ASUS Predator), operating at a refresh rate of 100 Hz. Participants began each trial by clicking the left mouse button. At the beginning of each trial a crosshair appeared at the center of the screen. Participants were instructed to maintain fixation throughout the duration of a trial and to try to blink between trials (i.e., withhold blinks during trials). After 500 ms, two memory items were presented (duration = 500 ms), one to the left and one to the right of central fixation (i.e., 4 degrees from central fixation). The two memory items, each with a diameter of 4 degrees, were differently oriented (i.e., horizontal, vertical, or diagonal) visual gratings (2.25 cycles per degree). A task-irrelevant flash event (duration = 100 ms) then occurred 300 ms after the presentation of the memory items, presented at the location of either of the previously presented memory items (with equal probability). Here, we hypothesized that the relative strength of the item representations (i.e., neural representations of the to-be-remembered items) would alternate in time as a function of oscillatory phase (Fig. 1D). We included the flash event to create a consistent pattern of alternation across trials (e.g., Item 1, Item 2, Item 1…)[37-39]. Following the flash event there was a variable memory delay, from 300–1600 ms. At the end of each trial, a memory probe (duration = 100 ms) was presented 4 degrees above central fixation. Participants reported, as quickly and as accurately as possible, whether the probe matched the memory item presented to (1) the left of fixation (40% of trials), (2) the right of fixation (40% of trials), or (3) neither of those memory items (20% of trials) by pressing 1, 2, or 3 on a keyboard. An auditory "ding" was presented when participants responded correctly. We defined 'Item 1' trials as those trials when the probe matched the memory item presented on the same side of fixation as the flash event, and 'Item 2' trials as

those trials when the probe matched the memory item presented on the opposite side of fixation from the flash event (Fig. 1B).

We tested whether response times (RTs) for correct trials differed depending on the Item condition (i.e., Item 1, Item 2, or Neither) and the Flash conditions (Right Flash or Left Flash) using a two-way repeated measures ANOVA and follow-up t tests. Based on the results of these statistical tests, we combined trials when the flash occurred on either the left or right of central fixation.

Data Acquisition and Pre-processing

Electroencephalographic (EEG) data were acquired with a 128-channel ActiveTwo BioSemi system (Amsterdam, the Netherlands), sampling at a rate of 512 Hz. For all analyses, we used a combination of customized MATLAB functions (The MathWorks, Natick, MA, USA) and the Fieldtrip toolbox (Donders Institute for Brain, Cognition, and Behaviour, Radbound University Nijmegen, the Netherlands)[59]. The EEG data were first zero-padded (2.5 seconds) and epoched (from 2.6 seconds before the memory probe to 0.8 seconds after the memory probe), then linearly detrended and demeaned. A discrete Fourier Transform (DFT) filter was used to remove 60-Hz line noise, and the data were re-referenced to the average of all 128 electrodes (i.e., we used an average reference). The data were visually inspected for each subject to determine a voltage threshold for removing all trials with artifacts associated with eye movements or blinks, using electrodes positioned near the eyes. For trials without evidence of eye movements or blinks, a threshold of ± 100 μV was used to identify trials with other noise transients[40]. The data at individual electrodes were interpolated, using the nearest neighbor spline[60], if fewer than 10% of electrodes were affected. Subjects who had artifacts on more than 20% of trials were excluded from all analyses (n = 5). The remaining subjects (n = 22) had an average of 8% of trials removed during artifact rejection, leaving an average of 880 trials per subject.

The present analyses were focused on frequency-specific phase during the memory delay (i.e., just prior to the memory probe). To measure phase on each trial, frequency-specific Morlet wavelets were used, with a varying number of cycles, from 2 cycles between 3 and 8 Hz, and increasing logarithmically from 2–5 cycles between 9 and 55 Hz. Each wavelet has a temporal extent based on the frequency and number of cycles. For example, a 4-Hz wavelet with 2 cycles extends for 500 ms. To limit the overlap between phase measurements and the evoked potential that occurred following the flash event, we only included trials where the memory delay was greater than 750 ms. For analyses measuring the relationship between frequency-specific phase and response times, the wavelet was fit for each frequency such that the last time point included in the phase measurement was the time point just prior to presentation of the memory probe. For the analysis of phase-amplitude coupling, wavelets for higher frequencies (i.e., 15–55 Hz) were centered at the same time point as the wavelet at 6 Hz (i.e., -167 ms). Pre-probe phase and

amplitude measurements were calculated based on the complex output of the wavelet convolution (i.e., taking either the angle or the absolute value).

Measuring Phase-Behavior and Phase-Amplitude Relationships

Here, we tested whether behavioral performance during a working memory task fluctuates as a function of oscillatory phase. To measure whether RTs were related to pre-probe phase (i.e., phase during the memory delay), RTs were first normalized for each participant by subtracting the mean of the RTs and dividing by the standard deviation of the RTs (i.e., we calculated z-standardized RTs). Here, trials with an RT less than 200 ms and trials with an RT greater than four standard deviations from the mean were excluded from further analysis[61]. For each condition (e.g., Item 1 and Item 2 combined, and Item 1 and Item 2 separately), RTs were binned based on frequency-specific pre-probe phase measurements (see the previous section for how we measured pre-probe phase), and average RTs were calculated in overlapping phase bins. The phase bins had a width of 90 degrees (e.g., 0–90 degrees) and were shifted forward in 10-degree steps (e.g., 10–100 degrees, then 20–110 degrees, etc.). This procedure was repeated to generate phase-RT functions, spanning all phases, for each frequency and each electrode. To capture consistent phase-RT relationships, these functions were averaged across participants (n = 22). Here, we predicted that the averaged phase-RT functions would have a signature shape, with a peak in RTs separated from a trough in RTs by approximately 180 degrees[28,40]. Based on this hypothesis, phase-RT functions were reduced to a single value for each frequency and electrode, using the following procedure: a discrete Fourier transform (DFT) was applied to each function (i.e., at each frequency and electrode) and the second component, representing a one-cycle sine wave (matching the hypothesized shape of the phase-detection relationship), was kept. The amplitude of this one-cycle, sinusoidal component—determined both by how closely the function approximated a one-cycle sine wave and by the effect size—was used to measure the strength of the phase-RT relationship[28,40] (Fig. 2A).

An identical procedure was used to test for a relationship between theta phase (at 6 Hz) and higher-frequency amplitude (i.e., phase-amplitude coupling) during the memory delay (i.e., just prior to the memory probe). Here, phase-amplitude functions (rather than phase-RT functions) were generated by binning higher-frequency amplitude (from 15–55 Hz) by theta phase, then averaging higher-frequency amplitude within the overlapping theta-phase bins[28]. Here, higher-frequency amplitudes were exclusively binned based on pre-probe theta phase from the electrode where we previously measured the strongest phase-RT relationship (Fig. 2).

For both the phase-behavior and the phase-amplitude analyses, statistical significance was determined by iteratively shuffling (5000 times) the trial-level phase measurements (breaking the relationship between either phase and behavior or phase and amplitude). For each iteration, the analysis steps were then repeated, using shuffled data to calculate the strength of the phase-RT

relationships or the phase-amplitude relationships. The resulting reference distributions (at each frequency and/or electrode) were compared to the magnitude of the observed data. For all analyses, before determining statistical significance, we controlled for the false discovery rate (accounting for multiple comparisons)[62].

Comparing Phase-RT Relationships Between Item Conditions

Here we predicted that the relative strength of the representations of different items should alternate in time as a function of oscillatory phase (Fig. 1D). We specifically tested whether the specific phases (from 3–55 Hz) associated with faster and slower RTs were different between the Item 1 and Item 2 conditions. Here, only electrodes where the phase-RT relationships exceeded a significance threshold of either $p < 0.05$ or $p < 0.1$ for both conditions (Fig. 2E) were included in the analysis. As described above, the discrete Fourier transform (DFT) was applied to each phase-RT function (see previous section) and the second component, representing a one-cycle sine wave, was kept. Here, the phase of the one-cycle sine waves (i.e., the angle of the second component), for each participant, were used (rather than the amplitudes). A circular Watson-Williams test[47] determined whether the phases ($n = 22$) of the one-cycle sine waves were statistically different for the Item 1 and Item 2 conditions (Fig. 3B). That is, whether faster and slower RTs for the Item 1 condition were associated with different phases than faster and slower RTs for the Item 2 condition.

ACKNOWLEDGMENTS

This work was supported by grants from the National Science Foundation (NSF 2120539) and the Searle Scholars Program to I.C.F. We would like to thank Dr. Edmund Lalor for inviting us to collect data in his laboratory while our own laboratory space was being renovated.

AUTHOR CONTRIBUTIONS

I.C.F. conceived of the experiment. M.A. and Z.V.R. collected data. I.C.F analyzed the data. I.C.F wrote the first draft of the manuscript. I.C.F., M.A., and Z.V.R. edited the manuscript.

DECLARATION OF INTERESTS

The authors declare no competing interests.

REFERENCES

1. Moore, T., and Zirnsak, M. (2017). Neural Mechanisms of Selective Visual Attention. Annual review of psychology *68*, 47-72. 10.1146/annurev-psych-122414-033400.
2. Fiebelkorn, I.C., and Kastner, S. (2020). Functional Specialization in the Attention Network. Annual review of psychology *71*, 221-249. 10.1146/annurev-psych-010418-103429.

3. Fiebelkorn, I.C., and Kastner, S. (2019). A Rhythmic Theory of Attention. Trends in cognitive sciences *23*, 87-101. 10.1016/j.tics.2018.11.009.
4. Benedetto, A., Morrone, M.C., and Tomassini, A. (2019). The common rhythm of action and perception. Journal of cognitive neuroscience *32*, 187-200. 10.1162/jocn_a_01436.
5. Baddeley, A. (1992). Working memory. Science *255*, 556-559. 10.1126/science.1736359.
6. Panichello, M.F., and Buschman, T.J. (2021). Shared mechanisms underlie the control of working memory and attention. Nature *592*, 601-605. 10.1038/s41586-021-03390-w.
7. Warden, M.R., and Miller, E.K. (2007). The representation of multiple objects in prefrontal neuronal delay activity. Cerebral cortex *17 Suppl 1*, i41-50. 10.1093/cercor/bhm070.
8. Rigotti, M., Barak, O., Warden, M.R., Wang, X.J., Daw, N.D., Miller, E.K., and Fusi, S. (2013). The importance of mixed selectivity in complex cognitive tasks. Nature *497*, 585-590. 10.1038/nature12160.
9. Constantinidis, C., Funahashi, S., Lee, D., Murray, J.D., Qi, X.L., Wang, M., and Arnsten, A.F.T. (2018). Persistent Spiking Activity Underlies Working Memory. The Journal of neuroscience : the official journal of the Society for Neuroscience *38*, 7020-7028. 10.1523/JNEUROSCI.2486-17.2018.
10. Fuster, J.M., and Alexander, G.E. (1971). Neuron activity related to short-term memory. Science *173*, 652-654. 10.1126/science.173.3997.652.
11. Goldman-Rakic, P.S. (1995). Cellular basis of working memory. Neuron *14*, 477-485. 10.1016/0896-6273(95)90304-6.
12. Miller, E.K., Lundqvist, M., and Bastos, A.M. (2018). Working Memory 2.0. Neuron *100*, 463-475. 10.1016/j.neuron.2018.09.023.
13. Kaminski, J., and Rutishauser, U. (2020). Between persistently active and activity-silent frameworks: novel vistas on the cellular basis of working memory. Ann N Y Acad Sci *1464*, 64-75. 10.1111/nyas.14213.
14. Lundqvist, M., Herman, P., and Miller, E.K. (2018). Working Memory: Delay Activity, Yes! Persistent Activity? Maybe Not. The Journal of neuroscience : the official journal of the Society for Neuroscience *38*, 7013-7019. 10.1523/JNEUROSCI.2485-17.2018.
15. Stokes, M.G. (2015). 'Activity-silent' working memory in prefrontal cortex: a dynamic coding framework. Trends in cognitive sciences *19*, 394-405. 10.1016/j.tics.2015.05.004.
16. Lundqvist, M., Rose, J., Herman, P., Brincat, S.L., Buschman, T.J., and Miller, E.K. (2016). Gamma and Beta Bursts Underlie Working Memory. Neuron *90*, 152-164. 10.1016/j.neuron.2016.02.028.
17. Lisman, J.E., and Idiart, M.A. (1995). Storage of 7 +/- 2 short-term memories in oscillatory subcycles. Science *267*, 1512-1515.
18. Siegel, M., Warden, M.R., and Miller, E.K. (2009). Phase-dependent neuronal coding of objects in short-term memory. Proceedings of the National Academy of Sciences of the United States of America *106*, 21341-21346. 10.1073/pnas.0908193106.
19. Bahramisharif, A., Jensen, O., Jacobs, J., and Lisman, J. (2018). Serial representation of items during working memory maintenance at letter-selective cortical sites. PLoS biology *16*, e2003805. 10.1371/journal.pbio.2003805.
20. Kaminski, J., Brzezicka, A., Mamelak, A.N., and Rutishauser, U. (2020). Combined Phase-Rate Coding by Persistently Active Neurons as a Mechanism for Maintaining Multiple Items in Working Memory in Humans. Neuron *106*, 256-264 e253. 10.1016/j.neuron.2020.01.032.
21. Caruso, V.C., Mohl, J.T., Glynn, C., Lee, J., Willett, S.M., Zaman, A., Ebihara, A.F., Estrada, R., Freiwald, W.A., Tokdar, S.T., and Groh, J.M. (2018). Single neurons may encode

simultaneous stimuli by switching between activity patterns. Nature communications *9*, 2715. 10.1038/s41467-018-05121-8.
22. Voloh, B., Oemisch, M., and Womelsdorf, T. (2019). Phase of Firing Coding of Learning Variables across Prefrontal Cortex, Anterior Cingulate Cortex and Striatum during Feature Learning. bioRxiv.
23. Buzsaki, G. (2002). Theta oscillations in the hippocampus. Neuron *33*, 325-340. 10.1016/s0896-6273(02)00586-x.
24. O'Keefe, J., and Recce, M.L. (1993). Phase relationship between hippocampal place units and the EEG theta rhythm. Hippocampus *3*, 317-330. 10.1002/hipo.450030307.
25. Reddy, L., Self, M.W., Zoefel, B., Poncet, M., Possel, J.K., Peters, J.C., Baayen, J.C., Idema, S., VanRullen, R., and Roelfsema, P.R. (2021). Theta-phase dependent neuronal coding during sequence learning in human single neurons. Nature communications *12*, 4839. 10.1038/s41467-021-25150-0.
26. Jun, N.Y., Ruff, D.A., Kramer, L.E., Bowes, B., Tokdar, S.T., Cohen, M.R., and Groh, J.M. (2022). Coordinated multiplexing of information about separate objects in visual cortex. eLife *11*. 10.7554/eLife.76452.
27. Helfrich, R.F., Fiebelkorn, I.C., Szczepanski, S.M., Lin, J.J., Parvizi, J., Knight, R.T., and Kastner, S. (2018). Neural mechanisms of sustained attention are rhythmic. Neuron *99*, 829-841. 10.1016/j.neuron.2018.07.032.
28. Fiebelkorn, I.C., Pinsk, M.A., and Kastner, S. (2018). A dynamic interplay within the frontoparietal network underlies rhythmic spatial attention. Neuron *99*, 842-853. 10.1016/j.neuron.2018.07.038.
29. Schroeder, C.E., Wilson, D.A., Radman, T., Scharfman, H., and Lakatos, P. (2010). Dynamics of Active Sensing and perceptual selection. Current opinion in neurobiology *20*, 172-176. 10.1016/j.conb.2010.02.010.
30. D'Esposito, M., and Postle, B.R. (2015). The cognitive neuroscience of working memory. Annual review of psychology *66*, 115-142. 10.1146/annurev-psych-010814-015031.
31. Funahashi, S., Bruce, C.J., and Goldman-Rakic, P.S. (1989). Mnemonic coding of visual space in the monkey's dorsolateral prefrontal cortex. Journal of neurophysiology *61*, 331-349. 10.1152/jn.1989.61.2.331.
32. Fusi, S., Miller, E.K., and Rigotti, M. (2016). Why neurons mix: high dimensionality for higher cognition. Current opinion in neurobiology *37*, 66-74. 10.1016/j.conb.2016.01.010.
33. Jones, S.R. (2016). When brain rhythms aren't 'rhythmic': implication for their mechanisms and meaning. Current opinion in neurobiology *40*, 72-80. 10.1016/j.conb.2016.06.010.
34. Lisman, J.E., and Jensen, O. (2013). The theta-gamma neural code. Neuron *77*, 1002-1016. 10.1016/j.neuron.2013.03.007.
35. Sternberg, S. (1966). High-speed scanning in human memory. Science *153*, 652-654. 10.1126/science.153.3736.652.
36. Ray, S., and Maunsell, J.H. (2011). Different origins of gamma rhythm and high-gamma activity in macaque visual cortex. PLoS biology *9*, e1000610. 10.1371/journal.pbio.1000610.
37. Landau, A.N., and Fries, P. (2012). Attention samples stimuli rhythmically. Current biology : CB *22*, 1000-1004. 10.1016/j.cub.2012.03.054.
38. Wolff, M.J., Jochim, J., Akyurek, E.G., and Stokes, M.G. (2017). Dynamic hidden states underlying working-memory-guided behavior. Nature neuroscience *20*, 864-871. 10.1038/nn.4546.

39. Wolff, M.J., Ding, J., Myers, N.E., and Stokes, M.G. (2015). Revealing hidden states in visual working memory using electroencephalography. Frontiers in systems neuroscience *9*, 123. 10.3389/fnsys.2015.00123.
40. Fiebelkorn, I.C., Snyder, A.C., Mercier, M.R., Butler, J.S., Molholm, S., and Foxe, J.J. (2013). Cortical cross-frequency coupling predicts perceptual outcomes. NeuroImage *69*, 126-137. 10.1016/j.neuroimage.2012.11.021.
41. Fiebelkorn, I.C., Pinsk, M.A., and Kastner, S. (2019). The mediodorsal pulvinar coordinates the macaque fronto-parietal network during rhythmic spatial attention. Nature communications *10*, 215. 10.1038/s41467-018-08151-4.
42. Cavanagh, J.F., and Frank, M.J. (2014). Frontal theta as a mechanism for cognitive control. Trends in cognitive sciences *18*, 414-421. 10.1016/j.tics.2014.04.012.
43. Ratcliffe, O., Shapiro, K., and Staresina, B.P. (2022). Fronto-medial theta coordinates posterior maintenance of working memory content. Current biology : CB *32*, 2121-2129 e2123. 10.1016/j.cub.2022.03.045.
44. Hsieh, L.T., and Ranganath, C. (2014). Frontal midline theta oscillations during working memory maintenance and episodic encoding and retrieval. NeuroImage *85 Pt 2*, 721-729. 10.1016/j.neuroimage.2013.08.003.
45. Schmidt, R., Herrojo Ruiz, M., Kilavik, B.E., Lundqvist, M., Starr, P.A., and Aron, A.R. (2019). Beta Oscillations in Working Memory, Executive Control of Movement and Thought, and Sensorimotor Function. The Journal of neuroscience : the official journal of the Society for Neuroscience *39*, 8231-8238. 10.1523/JNEUROSCI.1163-19.2019.
46. Scheeringa, R., Petersson, K.M., Oostenveld, R., Norris, D.G., Hagoort, P., and Bastiaansen, M.C. (2009). Trial-by-trial coupling between EEG and BOLD identifies networks related to alpha and theta EEG power increases during working memory maintenance. NeuroImage *44*, 1224-1238. 10.1016/j.neuroimage.2008.08.041.
47. VanRullen, R. (2016). How to Evaluate Phase Differences between Trial Groups in Ongoing Electrophysiological Signals. Frontiers in neuroscience *10*, 426. 10.3389/fnins.2016.00426.
48. Canolty, R.T., and Knight, R.T. (2010). The functional role of cross-frequency coupling. Trends in cognitive sciences *14*, 506-515. 10.1016/j.tics.2010.09.001.
49. Jensen, O., and Colgin, L.L. (2007). Cross-frequency coupling between neuronal oscillations. Trends in cognitive sciences *11*, 267-269. 10.1016/j.tics.2007.05.003.
50. Donoghue, T., Haller, M., Peterson, E.J., Varma, P., Sebastian, P., Gao, R., Noto, T., Lara, A.H., Wallis, J.D., Knight, R.T., et al. (2020). Parameterizing neural power spectra into periodic and aperiodic components. Nature neuroscience *23*, 1655-1665. 10.1038/s41593-020-00744-x.
51. Tsujimoto, T., Shimazu, H., and Isomura, Y. (2006). Direct recording of theta oscillations in primate prefrontal and anterior cingulate cortices. Journal of neurophysiology *95*, 2987-3000. 10.1152/jn.00730.2005.
52. Brzezicka, A., Kaminski, J., Reed, C.M., Chung, J.M., Mamelak, A.N., and Rutishauser, U. (2019). Working Memory Load-related Theta Power Decreases in Dorsolateral Prefrontal Cortex Predict Individual Differences in Performance. Journal of cognitive neuroscience *31*, 1290-1307. 10.1162/jocn_a_01417.
53. Riddle, J., Scimeca, J.M., Cellier, D., Dhanani, S., and D'Esposito, M. (2020). Causal Evidence for a Role of Theta and Alpha Oscillations in the Control of Working Memory. Current biology : CB *30*, 1748-1754 e1744. 10.1016/j.cub.2020.02.065.
54. Johnson, E.L., Dewar, C.D., Solbakk, A.K., Endestad, T., Meling, T.R., and Knight, R.T. (2017). Bidirectional Frontoparietal Oscillatory Systems Support Working Memory. Current biology : CB *27*, 1829-1835 e1824. 10.1016/j.cub.2017.05.046.

55. Buschman, T.J., Siegel, M., Roy, J.E., and Miller, E.K. (2011). Neural substrates of cognitive capacity limitations. Proceedings of the National Academy of Sciences of the United States of America *108*, 11252-11255. 10.1073/pnas.1104666108.
56. Salazar, R.F., Dotson, N.M., Bressler, S.L., and Gray, C.M. (2012). Content-specific fronto-parietal synchronization during visual working memory. Science *338*, 1097-1100. 10.1126/science.1224000.
57. Jacob, S.N., Hahnke, D., and Nieder, A. (2018). Structuring of Abstract Working Memory Content by Fronto-parietal Synchrony in Primate Cortex. Neuron *99*, 588-597 e585. 10.1016/j.neuron.2018.07.025.
58. Antzoulatos, E.G., and Miller, E.K. (2016). Synchronous beta rhythms of frontoparietal networks support only behaviorally relevant representations. eLife *5*. 10.7554/eLife.17822.
59. Oostenveld, R., Fries, P., Maris, E., and Schoffelen, J.M. (2011). FieldTrip: Open source software for advanced analysis of MEG, EEG, and invasive electrophysiological data. Computational intelligence and neuroscience *2011*, 156869. 10.1155/2011/156869.
60. Perrin, F., Pernier, J., Bertrand, O., Giard, M.H., and Echallier, J.F. (1987). Mapping of scalp potentials by surface spline interpolation. Electroencephalography and clinical neurophysiology *66*, 75-81. 10.1016/0013-4694(87)90141-6.
61. Su, Z., Wang, L., Kang, G., and Zhou, X. (2021). Reward makes the rhythmic sampling of spatial attention emerge earlier. Attention, perception & psychophysics *83*, 1522-1537. 10.3758/s13414-020-02226-5.
62. Benjamini, Y., and Yekutieli, D. (2001). The control of the false discovery rate in multiple testing under dependency. Ann Stat *29*, 1165-1188. 10.1214/aos/1013699998.